1 IEEE CICC 2022

Wireless, Batteryless, and Secure Implantable Systemon-a-Chip for 1.37mmHg Strain Sensing with Bandwidth Reconfigurability for Cross-Tissue Adaptation

M. R. Abdelhamid, U. Ha, U. Banerjee*, F. Adib, A. Chandrakasan Massachusetts Institute of Technology, *Indian Institute of Science

There is a growing interest in wireless and batteryless implants for long-term sensing of organ movements, core pressure, glucose levels, or other biometrics [1]. Most research on such implants has focused on ultrasonic [2] and nearfield inductive [3-4] methods for power and communication, which require direct contact or close proximity (<1-5cm) to the human body. Recently, RF backscatter has emerged as a promising alternative due to its ability to communicate with far-field (> 10cm) wireless devices at ultra-low-power [5]. While multiple proposals have demonstrated far-field RF backscatter in deep tissues, these proposals have been limited to tag identification and could neither perform biometric sensing nor secure the wireless communication links, which is critical for ensuring the confidentiality of the sensed biometrics and for responding to commands only from authorized users [6]. Moreover, such far-field RF implants are susceptible to tissue variations which impact their resonance and hence their efficiency in RF backscatter and energy harvesting.

This paper presents a wireless, batteryless, and secure implantable system-on-a-chip with integrated strain sensing as conceptually illustrated in Fig. 1 by: 1) designing a fully reconfigurable implantable rectenna that can adapt its center frequency and bandwidth to enable more efficient energy harvesting and backscatter communication across different tissues; 2) developing a highly efficient strain sensing front-end (5.9 mmHg·nJ/conv.) that enables high-resolution (1.37 mmHg), high-dynamic range (0-2000 mmHg) strain sensing; 3) co-designing an ultra-low-power AES security engine with the sensor interface to optimize area-efficiency via ADC sharing, while enabling confidentiality and authentication of sensed biometrics; 4) utilizing over-the-air closed-loop wireless programming to enable RF-front adaptation to surrounding tissues as well as fast settling time of the sensor front-end (<2s vs 2min without over-the-air programming).

The overall system and block diagram of the chip are shown in Fig. 2. A wireless device transmits a downlink signal in the 900MHz UHF ISM band to power up the chip and command it to initiate in-body sensing or to reconfigure its RF/sensor front-ends. The chip rectifies the RF signal to provide a 0.55V stable supply for the receiver chain, security engine, sensor front-end, and transmitter. The receiver chain couples the envelope of the RF signal into a baseband amplifier followed by an integrate-and-dump decoder for the Pulse Interval Encoded (PIE) input bits. A correlator detects the node ID in the preamble and enables the security engine with a pre-shared key to authenticate and decrypt the downlink command through an onchip AES Galois/Counter mode engine (AES-128-GCM) [7]. Once authenticated, a piezoelectric strain sensor feeds the sensor frontend with in-body measurements which are buffered and encrypted using an initialization vector (IV) from an on-chip true random number generator (TRNG). The uplink encrypted payload is packed with bursts of sensor data as well as internal states, and is transmitted via FM0-encoded backscatter at data rates up to 6Mbps.

Fig. 3 depicts the detailed operation protocol of the chip and the reconfigurable rectenna. The rectenna design consists of microstrip loops with programmable coupling. The outer structure is loaded with a switched capacitor bank to tune the antenna's impedance and quality factor to the surrounding medium's dielectric, while the inner loop connects to a programmable capacitor bank which provides impedance tunability for optimal harvesting efficiency. Different capacitive loading alters the overall current distribution in the antenna as shown in the EM simulations of Fig. 3, which enables increasing its effective area for harvesting and backscatter SNR across tissues. In comparison to previous programmable rectennas in RF backscatter where only the resonance frequency can be changed [5], this chip can also adapt its Q-factor by a factor of 8 to optimize for higher efficiency or higher bandwidth datarate. This is due to two innovations: the first is the Q-programmable antenna and matching design. The second is that, unlike prior designs, the system can perform adaptive reconfiguration via closed-loop over-the-air programming. After authenticating a reconfiguration command, the node backscatters an ACK to the reader which can repeatedly estimate the SNR of the ACK packet and send updated parameters to reconfigure the input matching (C_m), the antenna load (C₁), and the backscatter rate. After converging to optimal parameters for high-SNR, it sends a downlink command to initiate strain sensing.

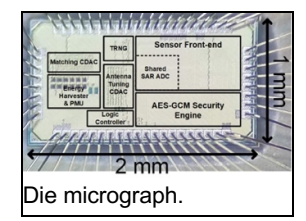


Fig. 4 shows the sensor front-end with ADC sharing. The front-end consists of a low noise amplifier (LNA), programmable gain amplifier (PGA), and a 10-bit SAR ADC. A digital accumulator closes the sensor loop to provide large DC cancellation and extract the small signal strain perturbations with a 1.37mmHg resolution for long term monitoring. While the high gain low-noise low-bandwidth amplification achieves high sensitivity, the large DC component strongly loads the cancellation loop requiring around 8 minutes to settle. The digital accumulator implements a programmable threshold to trade-off cancellation accuracy with settling time scaling it down to 40 seconds. Furthermore, an over-the-air programming scheme is demonstrated where the chip sends the latest DAC configurations in the uplink packets, allowing the transmit node to provide an initial DC-preset for the cancellation loop and scaling the settling time down to 2 seconds only. Additionally, the 10-bit SAR ADC is shared between the sense amplifiers and a chaos-map TRNG which implements a dyadic transformation through refeeding back the residue of a single 1.5-bit multiplying DAC pipeline stage. The TRNG provides a discrete-time analog voltage which is quantized and buffered as a 96-bit IV for the encryption protocol.

The chip was tested in a wireless setup to evaluate the wireless reconfigurability across tissues, as shown in Fig. 5. Without reconfigurability, the chip could not harvest sufficient voltage within the UHF ISM band to power-up across tissues (<0.7V min threshold to power up). In contrast, the incorporation of reconfigurability enables boosting the efficiency by shifting resonance to the 900MHz ISM band for power-up within FCC regulations. Moreover, different configurations of C_m and C_t can be used to tune the backscattering bandwidth from 10MHz to 80MHz, which allows shifting between high-efficiency (high-Q) mode and higher-bandwidth (low-Q) to adapt for larger depth or throughput respectively based on available power. In-air measurements demonstrate the extent of resonance adaptation by shifting the center frequency up to 300MHz. While the different blocks operate sequentially, the overall active power at yields that the security engine is the most power-hungry block at 4.8µW. Time-domain waveforms measurements are provided to demonstrate authentication, encoding, and transmission.

Fig. 6 shows an ex-vivo wireless evaluation setup for strain sensing of a porcine stomach. A pump is used to induce motion in the stomach, which is measured using a commercial piezoelectric strain sensor interfaced with the antenna board and SoC laminated on the outer wall. The RF far-field backscatter enables the chip to power up and communicate at >15cm of distance. This design operates from a harvested regulated voltage of 0.55V supply and consumes 11µW active power while operating the ADC front-end at a sampling rate of 385Hz. While providing a wide sensing range of 0-2000mmHg, the proposed front-end achieves a long-term resolution of 1.37mmHg. In comparison to prior far-field implantables, it introduces bandwidth reconfigurability and over-the-air-programming; it is also the first to incorporate far-field operation, strain sensing, and security within the harvested power budget. The 2mm² chip was fabricated in a 65nm CMOS process as shown in the die photo. In conclusion, the paper presented the design, implementation, and evaluation of a wireless, batteryless, and secure microimplant that can enable a new generation of long-term biomedical sensing.

References:

- [1] H. Rahmani et al., IEEE JSSC, pp. 3177-3190, Oct. 2021.
- [2] S. Sonmezoglu et al., IEEE ISSCC, pp. 454-456, 2020.
- [3] J. Thimot et al., IEEE CICC, pp. 1-4, 2020.
- [4] P. Cong et al., IEEE ISSCC, pp. 428-429, 2009.
- [5] M. R. Abdelhamid et al., ACM MobiCom, pp. 1-14, 2020.
- [6] C. S. Juvekar et al., IEEE ISSCC, pp. 290-291, 2016.
- [7] U. Banerjee et al., IEEE ISSCC, pp. 42-44, 2018.

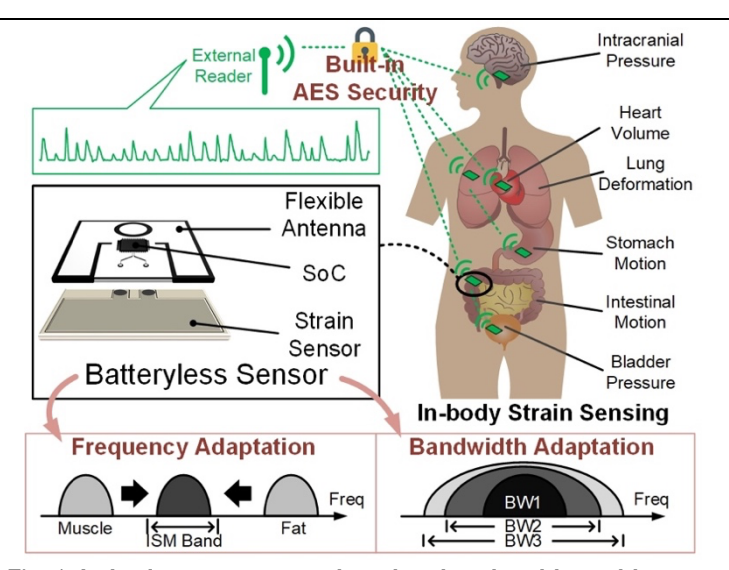


Fig. 1. In-body pressure sensing showing the chip architecture composed of the power management, communication, sensor front-end, and security engine circuits.

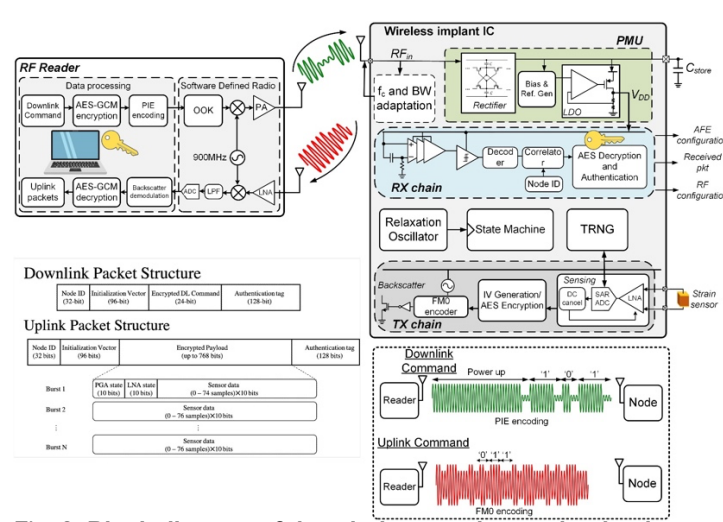


Fig. 2. Block diagram of the wireless strain sensing implant showing the different system blocks, modulation schemes, and the custom packet structures for the uplink and downlink communication.

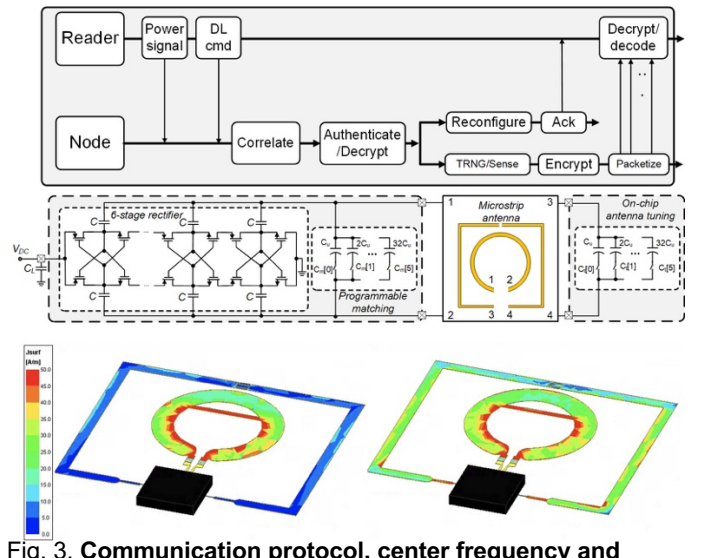


Fig. 3. Communication protocol, center frequency and bandwidth reconfigurability circuits showing antenna EM simulations at different configurations.

Center frequency tuning

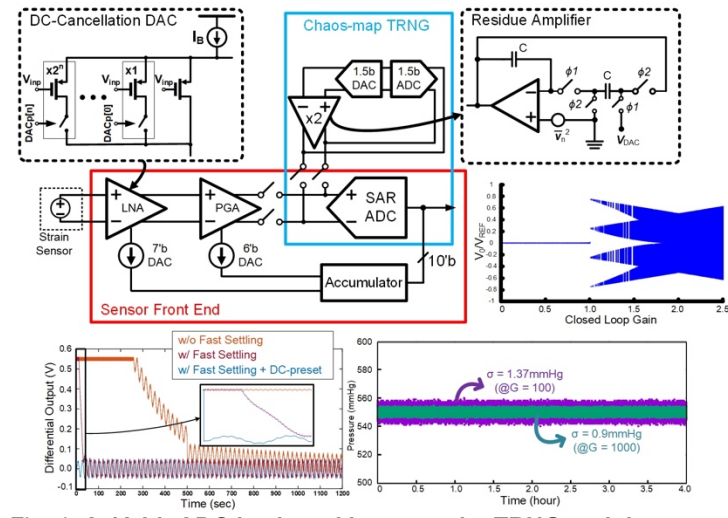


Fig. 4. A 10-bit ADC is shared between the TRNG and the analog sensor front end with a closed loop fast settling DC cancellation and achieving a 1.37mmHg long term stability.

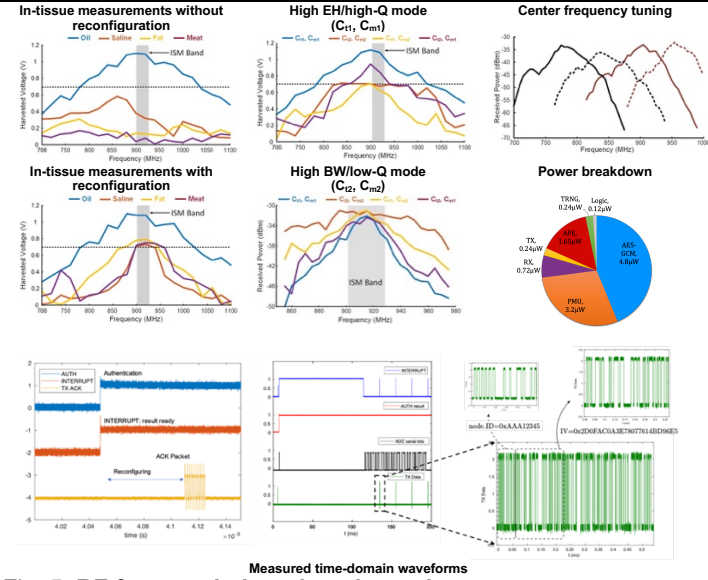


Fig. 5. RF front-end, time-domain, and power measurements across configurations and tissues.

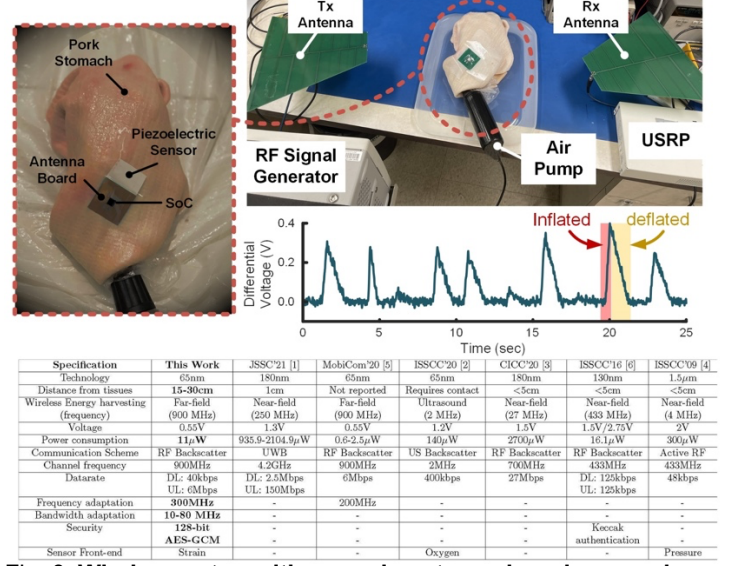


Fig. 6. Wireless setup with a porcine stomach and comparison to the state-of-the-art wireless batteryless sensing nodes